

Functional topographic organization of the motor reticulothalamic pathway

Ying-Wan Lam and S. Murray Sherman

J Neurophysiol 113:3090-3097, 2015. First published 25 February 2015; doi:10.1152/jn.00847.2014

You might find this additional info useful...

This article cites 25 articles, 11 of which can be accessed free at:

</content/113/9/3090.full.html#ref-list-1>

Updated information and services including high resolution figures, can be found at:

</content/113/9/3090.full.html>

Additional material and information about *Journal of Neurophysiology* can be found at:

<http://www.the-aps.org/publications/jn>

This information is current as of May 7, 2015.

Functional topographic organization of the motor reticulothalamic pathway

Ying-Wan Lam and S. Murray Sherman

Department of Neurobiology, University of Chicago, Chicago, Illinois

Submitted 27 October 2014; accepted in final form 5 February 2015

Lam YW, Sherman SM. Functional topographic organization of the motor reticulothalamic pathway. *J Neurophysiol* 113: 3090–3097, 2015. First published February 25, 2015; doi:10.1152/jn.00847.2014.—The thalamic reticular nucleus (TRN) is a thin layer of GABAergic cells lying rostral and lateral to the dorsal thalamus, and its projection to thalamic relay cells (i.e., the reticulothalamic pathway) strongly inhibits these cells. In an attempt to extend earlier studies of reticulothalamic connections to sensory thalamic nuclei, we used laser-scanning photostimulation to study the reticulothalamic projections to the main motor thalamic relays, the ventral anterior and lateral (VA and VL) nuclei, as well as to the nearby central lateral (CL) thalamic nucleus. VA/VL and the earlier studied somatosensory thalamic nuclei are considered “core” nuclei with topographic thalamocortical projections, whereas CL is thought to be a “matrix” nucleus with diffuse thalamocortical projections. We found that the TRN input footprints to VA/VL and CL are spatially localized and topographic and generally conform to the patterns established earlier for the TRN projections to sensory thalamic relays. These remarkable similarities suggest similar organization of reticulothalamic pathways and TRN regulation of thalamocortical communication for motor and sensory systems and perhaps also for core and matrix thalamus. Furthermore, we found that VA/VL and CL shared overlapping TRN input regions, suggesting that CL may also be involved in the relay of motor information.

thalamus; thalamocortical; motor; thalamic reticular nucleus; photostimulation

THE THALAMIC RETICULAR NUCLEUS (TRN) is a thin band of GABAergic cells lying rostral and lateral to the relay nuclei of the dorsal thalamus. Axons of both thalamocortical relay cells and corticothalamic cells from cortical *layer 6* branch and innervate reticular neurons as they transverse the TRN. Both pathways excite reticular neurons strongly, which in turn also strongly inhibit the thalamus (Lam and Sherman 2005, 2010, 2011). Because of such circuit configuration, the TRN helps to control the flow of thalamocortical information through two mechanisms: a negative feedback inhibition in which the TRN neurons are activated by thalamic relay cells and a top-down, cortically driven TRN inhibition of relay cells originating with *layer 6* neurons.

We previously completed detailed studies of the functional organization of the reticulothalamic projection to the first order somatosensory relay, ventral posterior medial nucleus (VPM), and its higher order companion, the posterior medial nucleus (POm) (Lam and Sherman 2005, 2007, 2011); first order relays are defined as thalamic nuclei receiving their driving input from a subcortical source (e.g., retinal input to the lateral geniculate nucleus or medial lemniscal input to the VPM), whereas higher order relays receive much of their driving input

from *layer 5* of cortex (e.g., from primary somatosensory cortex to POm) and project to higher cortical areas (reviewed in Sherman and Guillery 2013), although some POm cells may also receive driving inputs from subcortical sources (Groh et al. 2013). We found that the TRN projections to both relay nuclei were topographic; however, the projection to the first order VPM was from smaller, single TRN zones, whereas that to the higher order POm involved larger and sometimes multiple zones. Based on these findings and the topography of the reticulothalamic pathway, we and others have suggested two additional mechanisms in which TRN could regulate thalamocortical information transmission: a lateral inhibition through which thalamic neurons suppress their immediate neighbors and a long-range intrathalamic inhibition through which they suppresses neurons in another nucleus through TRN (Crabtree et al. 1998; Crabtree and Isaac 2002; Lam et al. 2005; Lam and Sherman 2007).

To extend these principles beyond sensory systems, we performed similar studies of the reticulothalamic projections to the main motor thalamic relays, the ventral anterior and lateral (VA and VL), and the neighboring central lateral (CL) thalamic nuclei. In rats and mice, VA and VL are generally indistinguishable on cytoarchitectural grounds (Groenewegen and Witter 2004; Jones 2007) and thus often treated as one nucleus, which we refer to as VA/VL. It was, however, recently reported in rats that VA/VL can be divided into two zones, one the target of the basal ganglia and the other innervated by the deep cerebellar nuclei (Kuramoto et al. 2009, 2011), and a similar division has been reported for primates (reviewed in Jones 2007). It has also been suggested that the cerebellar target region of VA/VL constitutes a first order relay, whereas that of the basal ganglia target region is also innervated by *layer 5* of motor cortex, which suggests a higher order relay for this region (Sherman and Guillery 2013).

The CL seems to be organized in many ways differently from VA/VL and sensory thalamic nuclei. For instance, Jones (Jones 1998, 2001, 2007) has proposed that thalamic relays can be divided into core and matrix types, with the former providing topographic input mostly to middle cortical layers, whereas the latter provides a more diffuse projection, mostly to upper cortical layers. VA/VL and the sensory relays are examples of core nuclei, and CL is considered to be a matrix nucleus (Jones 1998, 2007). Very little is known about reticulothalamic relationships for matrix nuclei, which is why we added this to our experimental plan.

In brief, we found that the TRN projections to VA/VL and CL are topographic and generally conform to the patterns established earlier for the reticulothalamic projections to sensory thalamic relays.

Address for reprint requests and other correspondence: Y.-W. Lam, Dept. of Neurobiology, Univ. of Chicago, 947 E. 58th St., MC0926, Chicago, IL 60637 (e-mail: ywlam@uchicago.edu).

METHODS

Preparation of brain slices. Our procedures were approved by the Institutional Animal Care and Use Committee (IACUC) of the University of Chicago. Experiments were performed on slices taken from BALB/c mice (Harlan) of ages 10–15 days postnatal and of both sexes. Each animal was deeply anesthetized by inhalation of isoflurane, and its brain was quickly removed and chilled in ice-cold artificial cerebrospinal fluid (ACSF), which contained (in mM): 125 NaCl, 3 KCl, 1.25 NaH₂PO₄, 1 MgCl₂, 2 CaCl₂, 25 NaHCO₃, 25 glucose. Angles for slicing were first estimated from the Allen Atlas (<http://mouse.brain-map.org>) and optimized for the plane that provided maximal connectivity between TRN and VA/VL. In brief, brain blocks were cut at 45° off the midline on a 15° ramp (Fig. 1A), laid rostral side down, and then cut into 500 μm sections with a vibrating tissue slicer for physiological recording (Campden Instruments, Lafayette, IN). Figure 1B shows examples of the three slices that contain brain regions used as landmarks to identify relevant thalamic nuclei. The most rostral reticulothalamic slices were used in our studies, since, in our experience, they most commonly contained the intact VA/VL, CL, and mediodorsal (MD) nuclei (rightmost in Fig. 1, B and C) and their reticulothalamic inputs. These slices were transferred to a holding chamber containing continuously oxygenated ACSF and incubated at room temperature for at least 1 h before each experiment.

Digital reconstruction of images of the brain slices. We also developed a computer algorithm that digitally “slices” rat or mouse brains and serves as a visual aid for identification of thalamic nuclei in brain slices. Our results here, however, was based on the rat atlas by Paxinos and Watson (Paxinos and Watson 2004), because it is the most recent version of a rat or mouse brain atlas that provides high-resolution images in a conveniently convertible format. Moreover, the larger size of rat brains improves the resolution of the digitally generated images of the slices. In brief, each anatomical region defined in the atlas was assigned a “color tag” that has an RGB value encoding a unique identity number, and these color tags were used to color the images of coronal slices. The colors of the pixels in this image stack thus stored the identity of brain regions as a three-dimensional matrix. To reconstruct the image of a brain

slice, three-dimensional coordinates of all the pixels are calculated and color tags from the nearest points in this matrix will be copied.

In Fig. 1C, these color tags were replaced with more legible colors to show how well digital reconstruction using the rat brain atlas reproduced the shapes and locations of the TRN and relevant thalamic nuclei in the slices (regions outlined in Fig. 1B) cut in this experiment. The shapes and locations of these thalamic nuclei, as well as those of the hippocampus and cerebral cortex, were used as landmarks to identify VA/VL *in vitro*. The same algorithm reproduced a similar spatial layout of the slices using lower resolution images of coronal sections of the mouse brain (Allen Atlas, <http://mouse.brain-map.org>); thus, in practice, this approach proved adequate as a visual aid in guiding our physiological recording, even though, because of the difference between mouse and rat brains, this did not perfectly reproduce the spatial layout of mouse slices *in vitro*.

Physiological recording. Whole cell recordings were performed with a visualized slice setup (Cox and Sherman 2000; Lam et al. 2005). Recording pipettes were pulled from borosilicate glass capillaries, and had a tip resistance of 3–6 MΩ when filled with a low chloride intracellular solution (termed hereafter the “pipette solution”) containing the following (in mM): 127 K-gluconate, 3 KCl, 1 MgCl₂, 0.07 CaCl₂, 10 HEPES, 2 Na₂-ATP, 0.3 Na-GTP, 0.1 EGTA. The pH of the pipette solution was adjusted to 7.3 with KOH or gluconic acid, and the osmolality was 280–290 mOsm.

A few threads of nylon filaments, attached to a platinum wire slice holder, were used to secure the slices in the bath during the experiment. The slice was carefully placed during the experiment so that the nylon threads did not interfere with electrophysiological recording and photostimulation and perfused with ACSF at 27°C throughout the experiment. We recorded using an Axopatch 200B amplifier (Molecular Devices, Sunnyvale, CA). The cells were recorded in voltage-clamp mode at a holding potential of –45 mV. The chloride reversal potential of the pipette solution allows clear detection of inhibitory postsynaptic currents (IPSCs) at this –45 mV holding potential. The access resistance of the cells was constantly monitored throughout the

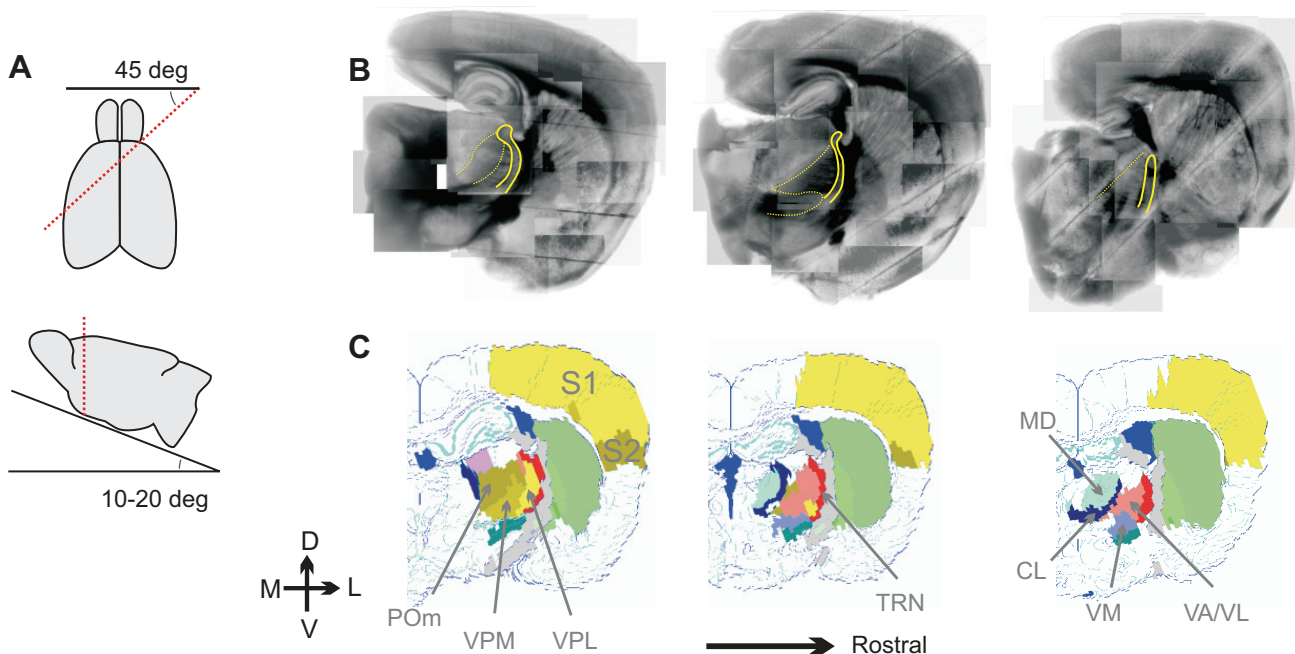


Fig. 1. A: schematic diagrams illustrating the brain slicing procedures. B: photomicrographs of the brain section containing relevant thalamic nuclei. Yellow lines highlight the border of TRN, which was used as a landmark for locating VA/VL. Yellow dotted lines indicate the border of relevant thalamic nuclei; see the labels below in D. C: digital reconstructions of the brain sections that are the most similar to those shown in B. POm, posterior medial nucleus; VPM, ventral posterior medial nucleus; VPL, ventral posterior lateral nucleus; TRN, thalamic reticular nucleus; MD, mediodorsal nucleus; CL, central lateral nucleus; VA/VL, ventral anterior and ventral lateral nucleus; VM, ventral medial nucleus; S1, primary somatosensory cortex.

recordings, and experiments were discontinued if this resistance exceeded 30 M Ω .

All chemicals were purchased from Sigma-Aldrich (St. Louis, MO) or Tocris (Bristol, UK).

Photostimulation. We used our previously described methods for photostimulation (Lam et al. 2006; Lam and Sherman 2005, 2007, 2010, 2011). Briefly, data acquisition and photostimulation were controlled by the program Tidalwave, written in Matlab (MathWorks, Natick, MA) by the laboratory of Karel Svoboda (Shepherd et al. 2003). Nitroindoliny (NI)-caged glutamate (Canepari et al. 2001) (Sigma-Aldrich, St. Louis, MO) was added to the recirculating ACSF to a concentration of 0.39 mM during recording. Focal photolysis of the caged glutamate was accomplished by a pulsed UV laser (355 nm wavelength, frequency-tripled Nd:YVO₄, 100 kHz pulse repetition rate; DPSS Laser, San Jose, CA). The laser beam was directed into the side port of a double-port tube (U-DPTS) on top of an Olympus microscope (BX50WI) using UV-enhanced aluminum mirrors (Thorlabs, Newton, NJ) and a pair of mirror-galvanometers (Cambridge Technology, Cambridge, MA) and then focused onto the brain slice using a low-magnification objective (4 \times 0.1 Plan, Olympus). Angles of the mirror galvanometers were computer controlled and determined the position stimulated by the laser. The Q-switch of the laser and a shutter (LS3-ZM2; Vincent Associate, Rochester, NY) controlled the timing of the laser pulse for stimulation.

A variable neutral density wheel (Edmund, Barrington, NJ) controlled the power of photostimulation at different levels during experiments by attenuating the intensity of the laser. A microscope coverslip in the laser path reflected a small portion of the laser onto a photodiode, and the current output from this photodiode was used to monitor the laser intensity during the experiment. The photodiode output was calibrated to the laser power at the back focal plane of the objective when we set up the optical equipment, using a power meter (Thorlabs, Newton, NJ).

The standard stimulation pattern used for mapping consisted of positions arranged in an 8 \times 24 or 16 \times 16 array. To avoid receptor desensitization, local caged-glutamate depletion, and possible excitotoxicity, stimulation of these positions were arranged in a sequence that maximized the spatial distance between consecutive trials.

The laser stimulus was 2 ms long and consisted of 200 pulses. We used the maximum power possible for our laser, which varied between 50 and 65 mW measured at the back focal plane, in our experiment. Since the transmittance of the objective for the UV laser was \sim 40%, the actual power of the laser reaching the slices was less than half of the values we state. In our experience, laser pulses at this power are more than enough to maximally excite the brain slices to evoke the largest extent of reticulothalamic footprints (Lam and Sherman 2005, 2007, 2010, 2011; Lam et al. 2006). The intertrial interval was between 1 and 2 s. A typical experiment lasted between $\frac{1}{2}$ and 1 h, and we did not see any change of the response amplitude or membrane resistance during experiments that suggested damage from phototoxicity.

Data analysis. Responses to photostimulation could be easily and best visually detected by their short latency and the presence of similar responses in adjacent stimulation locations. These responses were quantitatively analyzed using programs written in Matlab and Octave (<http://www.octave.org>). For data presentation, traces of the recording immediately after the laser pulse were superimposed on a photomicrograph of the slice (see RESULTS). The abovementioned traces were arranged into an 8 \times 24 or 16 \times 16 array and placed where the laser was focused during the stimulation.

The areas in the slices where TRN photostimulation evoked responses in the recorded thalamic neurons are referred as their reticulothalamic input "footprint." Centroids of the input footprints that consist of one single continuous area are estimated using an equation similar to the calculation of the center-of-mass.

$$x_c = \frac{\sum_i x_i R_i}{\sum_i R_i}$$

$$y_c = \frac{\sum_i y_i R_i}{\sum_i R_i}$$

The parameters x_c and y_c are the coordinates of the centroid, while x_i and y_i are the coordinates of all the stimulation sites. R_i is a value based on peak outward current of the recordings within the 150 ms interval after photostimulation and are calculated as

$$R_i = P_i \quad \text{if } P_i > \theta$$

$$R_i = 0 \quad \text{if } P_i \leq \theta$$

where θ is a fixed threshold value, 25 pA, a value selected so that these footprints matched closely with visually detected ones. Centroids for the reticulothalamic input footprints that consist of more than one region were calculated separately for each region. For comparison across experiments, the tip of the hippocampus (red stars in Fig. 3A) was used as a reference point to correct the coordinates of the centroids and recording sites in our analysis.

The footprint area was measured by counting the number of "pixels" where photostimulation evoked outward current larger than a threshold value (25 pA). Since each pixel is a 50 μ m square, total footprint area in square meters can be obtained by multiplying the number of pixels with 2.5×10^{-9} m².

RESULTS

Responses to laser-scanning photostimulation. We recorded from 30 VA/VL and 24 CL neurons. The reticulothalamic input footprints of each of these neurons were determined by stimulating in 192 positions, arranged in an 8 \times 24 array, within the TRN. The examples in Fig. 2 show the 150 ms voltage-clamp recordings immediately following photostimulation for each of the 192 positions, and these traces are arranged in an 8 \times 24 grid, with each response overlying the location of photostimulation. Since TRN photostimulation evoked large outward (hyperpolarizing) currents at the -45 mV holding potential we used, the reticulothalamic input footprints to the recorded cells can be visualize by noting where upward peaks (i.e., outward currents) are visible in the recordings. Responses in these regions are enclosed with colored rectangles and shown rescaled below in Fig. 2.

Figure 2, A and B, show example input footprints for two VA/VL neurons. For 23 of the 30 VA/VL neurons, the reticulothalamic input footprints consist of one spatially confined elliptical region (Fig. 2A), which is the pattern we have noted previously for the first order somatosensory thalamic relay (VPM/VPL; Lam and Sherman 2005, 2007, 2011). However, for seven of the 30 VA/VL neurons, we observed footprints consist of two footprint regions, separated by gaps where no response could be detected (Fig. 2B). The spatial organization of the reticulothalamic input footprints for CL neurons are similar, because most (21 of 24; not shown) consist of a single elliptical region, and three consist of more than one region (Fig. 2C).

Topography of the reticulothalamic input footprint to VA/VL and CL. Figure 3A shows the summary of the locations of all reticulothalamic inputs to VA/VL (Fig. 3A₁) and CL (Fig. 3A₂) neurons. The coordinates of the recording sites and their reticulothalamic inputs, measured from the tip of the hippocampus (red stars in Fig. 3A), are represented either as filled or half-filled (the latter if they have more than one reticulothalamic input) colored circles and triangles and connected to

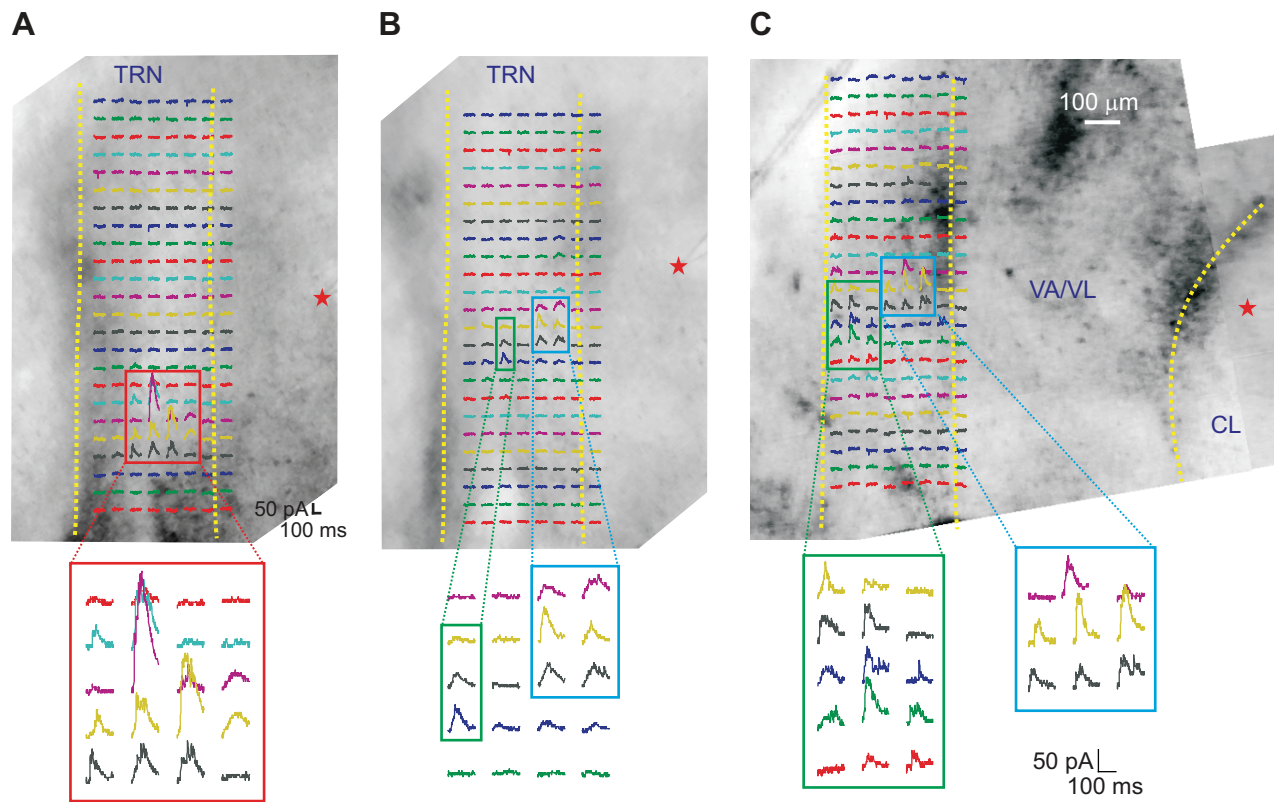


Fig. 2. Example responses of thalamic neurons to TRN photostimulation. In A–C, the red stars indicate the recording sites. The neurons were stimulated in TRN at 192 positions, arranged in an 8×24 matrix, and 150 ms of recordings immediately after photostimulation are shown where the laser was focused. **A:** TRN input footprint that consists of a single region. Regions where photostimulation evoked visible outward current are bordered (red) and shown below in a larger scale. **B:** TRN input footprint of a VA/VL neuron that consists of 2 regions. Outward current was evoked in 2 separated regions of the TRN (green and blue rectangles). **C:** example TRN input footprint of a CL neuron. Outward current could be evoked from 2 large regions of TRN (green and blue rectangles) in this neuron.

gether with colored lines. For reference, these plots are overlaid on top of a photomicrograph of the brain slice taken during one experiment, and yellow dotted lines in the photomicrographs indicate the approximate borders between thalamic nuclei. Even though some of the input footprints to CL appear to locate beyond the reticulothalamic border in Fig. 3A₂, it is likely to be an artifact due to the variation of the sizes and shapes of the TRN across experiments.

Data from Fig. 3A₁ and A₂ are combined together and plotted with the same colored symbols with larger scales in Fig. 3B. The locations of all the reticulothalamic inputs to the neurons of VA/VL and CL are plotted in Fig. 3B₁. It shows that the reticulothalamic inputs to these two nuclei occupy partially overlapped areas: the input to VA/VL occupies an outer tier that extends from the internal capsule to roughly two-thirds of the thickness of the TRN, whereas the input to CL occupies the inner two-thirds closer to the reticulothalamic border (Fig. 3B₁). Fig. 3B₂ shows the locations of all the neurons recorded in this study.

The dorsal-ventral coordinates (Fig. 3C, the vertical distance from the origin in Fig. 3A) and the lateral-medial coordinates (Fig. 3D, the horizontal distance from the origin) of the reticulothalamic inputs are plotted against the coordinates of the recording sites in Fig. 3, C and D. Correlations between the dorsal-ventral ($R = 0.572$, $n = 64$, $P < 0.001$, Pearson's correlation) and lateral-medial ($R = 0.536$, $n = 64$, $P < 0.001$, Pearson's correlation) coordinates were significant, suggesting topographic organization of these reticulothalamic projections.

Note that 10 of the neurons had two reticulothalamic inputs, therefore the value of n is 64 instead of 54.

Figure 3E plots the sizes of the reticulothalamic inputs to VA/VL and CL input against the lateral-medial coordinates of the recording sites. Averages are plotted as red (VA/VL, 11.5 ± 1.2 pixels, means \pm SE) and black (CL, 18.1 ± 2.4 pixels) stars. The average size of the inputs to CL neurons is significantly larger ($P = 0.0337$, $n = 24, 30$, Mann-Whitney test).

Disynaptic responses to laser-scanning photostimulation. Figure 4A, using the same format as Fig. 2, displays the results of an example experiment in which we recorded from a VA/VL neuron and stimulated at 256 positions over the thalamic region near the recording site. For this neuron, large inward (depolarizing) currents were evoked in a region with a roughly $200 \mu\text{m}$ diameter surrounding the recording site, an area similar in size to the dendritic arbors of rat and mouse thalamic neurons (Lam et al. 2005; Lee and Sherman). Since there is no excitatory interconnection between thalamic neurons, these inward currents could be only due to direct photostimulation of the soma and proximal dendrites. Beyond this region, large outward currents were evoked, which we previously demonstrated were blocked by the GABA antagonist, gabazine (Lam and Sherman 2005). Given the lack of local interneurons in VA/VL (Arcelli et al. 1997), these outward currents were presumably due to disynaptic activation via the TRN.

The same experiments were carried out for 28 VA/VL and nine CL neurons and similar disynaptic IPSCs were observed for all. Figure 4B shows the only case with a slightly different

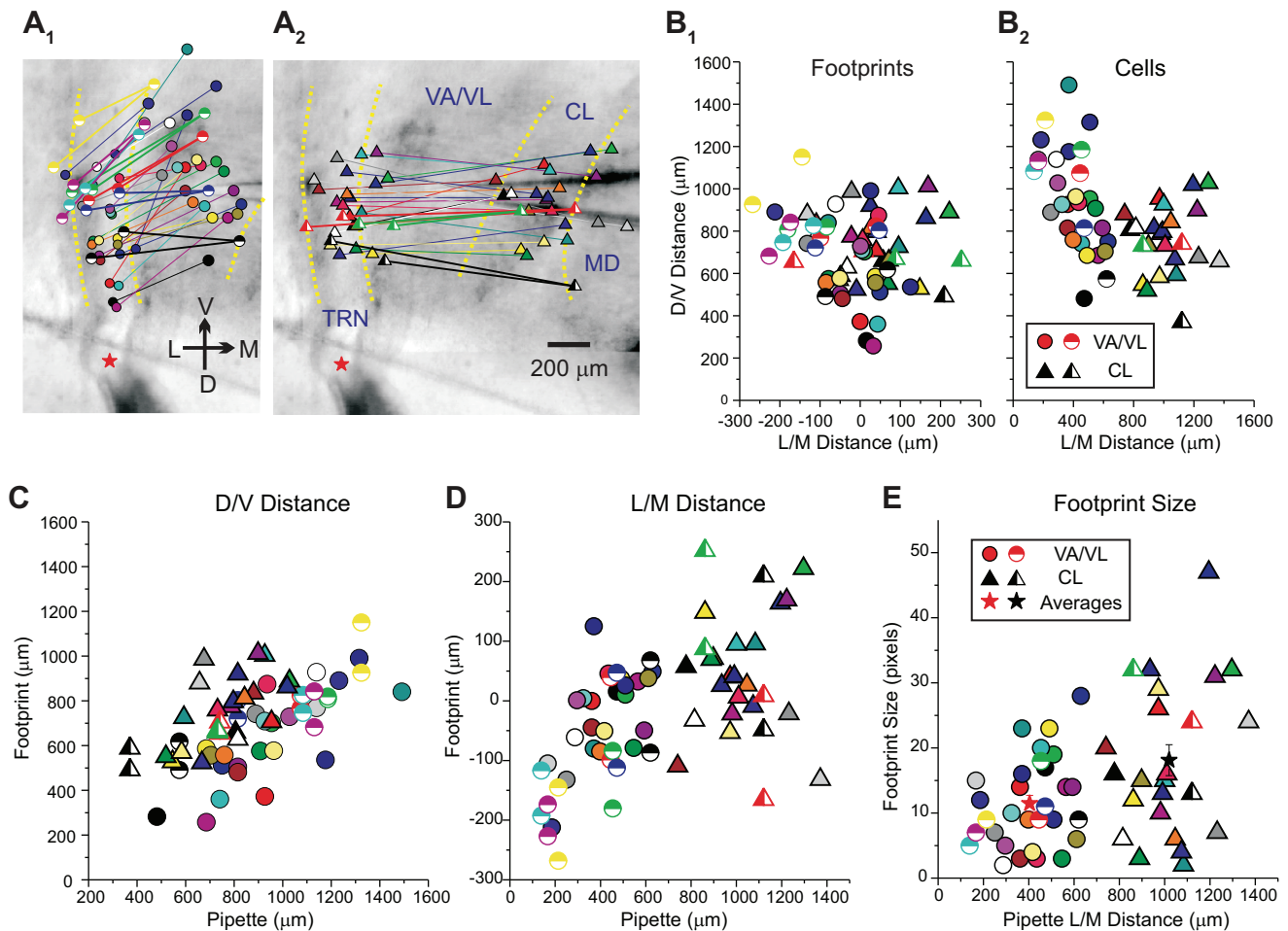


Fig. 3. Summary and analysis of the TRN input footprints to VA/VL and CL neurons. *A*: summary of all the input footprints to VA/VL (*A*₁) and CL (*A*₂) neurons. Locations of the recording sites and their reticulothalamic inputs are indicated by circles (*A*₁) and triangles (*A*₂) and connected with colored lines. Neurons with >1 input are represented with half-filled circles (*A*₁) and triangles (*A*₂). *B*: graphic plots of the locations of the input footprints (*B*₁) and recording sites (*B*₂). *C*, *D*: graphical analysis of the topography of the reticulothalamic pathway. Plots of the dorsal-ventral coordinates (*C*, vertical distance from the tip of the hippocampus, red stars in *A*₁ and *A*₂) and lateral-medial coordinates (*D*, horizontal distance from the tip of the hippocampus) of the reticulothalamic input against the coordinates of the recording sites. *E*: plot of the footprint size vs. the lateral-medial coordinates of the recording sites. Average sizes of the input footprints to VA/VL and CL are indicated with red (VA/VL) and black (CL) stars, respectively. Error bars represent standard errors. Data from the same experiments were represented with the same colors in all the figures.

result. As with the other experiments, photostimulation in this CL neuron evoked large inward current in the area immediately surrounding the stimulation site and disynaptic thalamo-reticulo-thalamic IPSCs at a further distance (blue rectangle). What is different is that, in this cell, photostimulation in a separated area in VA/VL also evoked IPSCs (green rectangle), suggesting disynaptic inhibition that involves TRN from VA/VL onto this CL neuron. The left inset of Fig. 4*B* displays the responses of this CL neuron to TRN photostimulation, and traces with detectable outward currents are enlarged below and to the left (yellow rectangle), showing the reticulothalamic input footprint of this neuron consisting of a large, though apparently continuous, area.

DISCUSSION

Functional organization of the motor reticulothalamic pathway. We studied the functional organization of the reticulothalamic input to VA/VL neurons with laser-scanning photostimulation. We found the input footprints of VA/VL neu-

rons are spatially localized (Fig. 2*A*) and topographic organized (Fig. 3, *C* and *D*). Such organization for these thalamic nuclei associated with the motor cortex is remarkably similar to that reported for VPM and POM of the somatosensory thalamus (Lam and Sherman 2005, 2007). Of interest is that the pattern of reticulothalamic footprints (i.e., the regions within the TRN that innervate a thalamic relay cell) were singular and smaller for the first-order VPM and somewhat larger and occasionally consist of multiple separate zones for the higher order POM (Lam and Sherman 2005, 2007). The range of footprints for VA/VL ran the gamut of those seen for VPM and POM, which is consistent with the idea that the VA/VL complex contains a mixture of cells, some that act as that first-order thalamic relays and others as higher order (Sherman and Guillery 2013).

This is consistent with evidence that VA/VL may contain two separate relay regions. For instance, in rats, VA/VL can be divided into two zones, one the target of the basal ganglia and the other innervated by the deep cerebellar nuclei (Kuramoto et al. 2009, 2011), and a similar division has been reported for

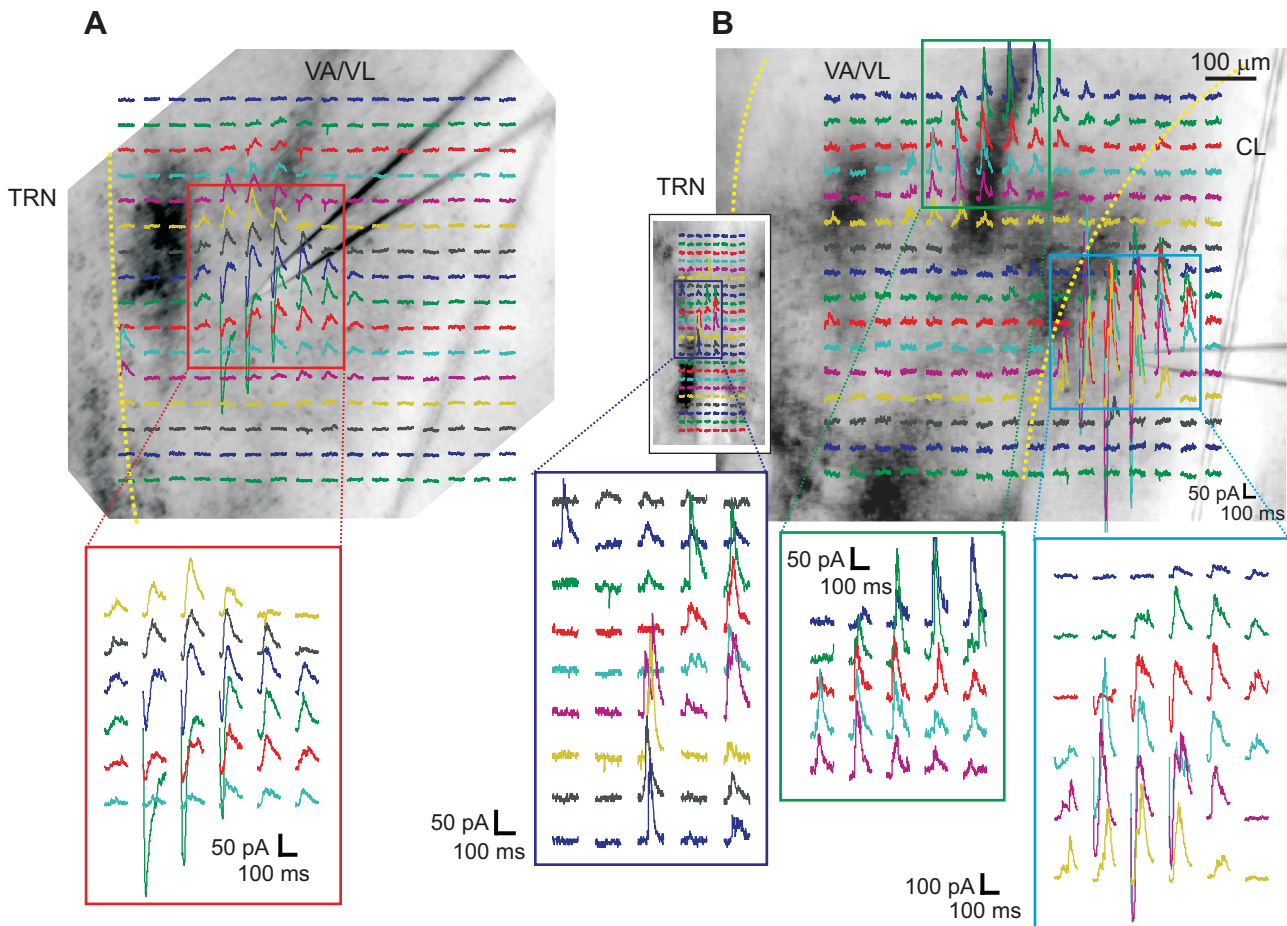


Fig. 4. Example responses of VA/VL and CL neurons to thalamic photostimulation. The neurons were stimulated in the thalamus at 256 positions, arranged in a 16×16 matrix, and the data are presented under the same format as Fig. 2. *A*: typical responses to thalamic photostimulation. Photostimulation evoked large inward current around the recording site and disynaptic thalamo-reticulo-thalamic inhibitory postsynaptic currents at a further distance. Responses near the recording sites are enlarged and shown below (red rectangle). *B*: one experiment in which the results were slightly different. Here, photostimulation evoked responses in 2 separated regions of the thalamus: one that surrounds the recording site (blue rectangle) and follows the same spatial patterns as the one shown in *A* and a 2nd one that is located in a different nucleus (green rectangle, VA/VL). Response traces in both regions are rescaled and shown below. *Inset* displays the responses of this neuron to TRN photostimulation, and responses with detectable outward currents are enlarged below (purple rectangle).

primates (reviewed in Jones 2007). Our results here, however, did not suggest any separation of VA and VL, either because they have overlapped TRN inputs or they are not distinguishable at the plane of sectioning we used.

The reticulothalamic footprints to CL, even though generally larger in area than those to VA/VL (Fig. 3*E*), are organized in a similar topography. CL is considered to be a matrix thalamic nucleus, which is thought to produce projections to cortex that are rather diffusely organized (Jones 1998, 2001, 2007), and so the topography seen in its inputs from TRN is notable. Another interesting result is the partially overlapped reticulothalamic inputs to VA/VL and CL (Fig. 3*B*). As TRN is commonly believed to be organized into functionally related sectors (Crabtree and Killackey 1989; FitzGibbon 2000; Jones 2007; Lozsadi 1994; Montero et al. 1977), our results suggest that either the organization of TRN may not be as strictly functionally divided as previously believed or CL neurons may be involved in the processing or modulation of motor information. Oculomotor-related activity has been reported for neurons within the CL, lateral dorsal, and MD nuclei of cats (Schlag et al. 1974) and monkeys (Schlag-Rey and Schlag 1984; Schlag and Schlag-Rey 1984). Our results are therefore consistent

with the possibility that, in addition to VA/VL, CL and a large portion of the thalamus is involved in the processing or modulation of motor information.

Because this study was conducted in slices, our experiments technically can reveal only the topography of the reticulothalamic pathway in the plane of the slice. Whereas we cannot rule out unusual patterns in, say, the perpendicular plane, this seems implausible, especially since the available evidence indicates that the plane we chose contains more of the projection than other planes, and the section thickness ($500 \mu\text{m}$) we used means that each slice we studied appear to contain most of VA/VL (see Fig. 1, *B* and *C*). We thus conclude that our results accurately reflect overall reticulothalamic topography.

Juvenile (10–15 days postnatal) animals were used in this experiment because VA/VL in older animals is optically much more opaque, making whole-cell recording quite difficult. Animals at this age already have overtly normal motor functions, and thus it seems unlikely, although possible, that the reticulothalamic circuits we have described are dramatically different in adult mice.

Inhibitory interactions between thalamic neurons. Similar to the somatosensory thalamus, stimulation of an area around the

somata evoked disynaptic IPSC responses in thalamic relay cells of VA/VL and CL. We interpreted this as evidence of TRN neurons receiving excitatory inputs from an area of thalamus that is larger than the targets of their reticular innervation and this circuit configuration provides a mechanism for “lateral inhibition” between neighboring thalamic neurons (Crabtree 1996; Lam and Sherman 2005, 2007). Similar results here for the motor thalamus suggest that the circuitry for such “lateral inhibition” is one of the general organization principles of reticulothalamic pathways.

Disynaptic IPSCs were evoked in one CL neuron from photostimulation of VA/VL (Fig. 4C). Similar disynaptic responses were observed in the somatosensory thalamus and were interpreted as evidence of involvement of TRN in mutual inhibition of neurons between different thalamic nuclei (Crabtree et al. 1998; Crabtree and Isaac 2002; Lam and Sherman 2007, 2011). What is surprising, however, is how rare this was: we found only one case in 37 experiments. Whether this is due to an angle of slicing that interferes more with these intrathalamic pathways in the studies reported here or less involvement of these pathways in motor processing is not clear.

Functional implications. The similarity in reticulothalamic projections to VA/VL and CL to that reported previously for sensory thalamic nuclei suggests a similar functional organization. That is, TRN controls the flow of information to cortex through these thalamic nuclei by providing a strong, specific, and topographic inhibitory input to relay cells, and this is largely under the control of the *layer 6* projection to the TRN (Lam and Sherman 2010). Previous studies of the connections between VA/VL and the motor cortex have focused on the indirect cortico-striato-pallidothalamic pathway (reviewed in Jones 2007; Sherman and Guillery 2013). Our results suggest additional pathways for which motor cortex modulates the relay of information it receives from thalamus in a topographic manner similar to that seen in the sensory cortices: through the *layer 6* corticothalamic projections that include both direct excitatory input to relay cells and indirect inhibition through the TRN.

Although more examples are needed, these results are also consistent with the simplifying notion that the TRN control of thalamocortical input is rather similar across thalamic nuclei, including both sensory and motor nuclei as well as core and matrix thalamic neurons.

GRANTS

This work was supported by National Institute on Deafness and Other Communication Disorders Grant DC-008794 and National Eye Institute Grant EY-022338.

DISCLOSURES

No conflicts of interest, financial or otherwise, are declared by the author(s).

AUTHOR CONTRIBUTIONS

Author contributions: Y.-W.L. and S.M.S. conception and design of research; Y.-W.L. performed experiments; Y.-W.L. and S.M.S. analyzed data; Y.-W.L. and S.M.S. interpreted results of experiments; Y.-W.L. and S.M.S. prepared figures; Y.-W.L. and S.M.S. drafted manuscript; Y.-W.L. and S.M.S. edited and revised manuscript; Y.-W.L. and S.M.S. approved final version of manuscript.

REFERENCES

- Arcelli P, Frassoni C, Regondi MC, De Biasi S, Spreafico R. GABAergic neurons in mammalian thalamus: a marker of thalamic complexity? *Brain Res Bull* 42: 27–37, 1997.
- Canepari M, Nelson L, Papageorgiou G, Corrie JE, Ogden D. Photochemical and pharmacological evaluation of 7-nitroindolyl- and 4-methoxy-7-nitroindolyl-amino acids as novel, fast caged neurotransmitters. *J Neurosci Meth* 112: 29–42, 2001.
- Cox CL, Sherman SM. Control of dendritic outputs of inhibitory interneurons in the lateral geniculate nucleus. *Neuron* 27: 597–610, 2000.
- Crabtree JW. Organization in the somatosensory sector of the cat's thalamic reticular nucleus. *J Comp Neurol* 366: 207–222, 1996.
- Crabtree JW, Collingridge GL, Isaac JT. A new intrathalamic pathway linking modality-related nuclei in the dorsal thalamus. *Nat Neurosci* 1: 389–394, 1998.
- Crabtree JW, Isaac JT. New intrathalamic pathways allowing modality-related and cross-modality switching in the dorsal thalamus. *J Neurosci* 22: 8754–8761, 2002.
- Crabtree JW, Killackey HP. The topographic organization and axis of projection within the visual sector of the rabbit's thalamic reticular nucleus. *Eur J Neurosci* 1: 94–109, 1989.
- FitzGibbon T. Cortical projections from the suprasylvian gyrus to the reticular thalamic nucleus in the cat. *Neuroscience* 97: 643–655, 2000.
- Groenewegen HJ, Witter MP. Thalamus. In: *The Rat Nervous System*, edited by Paxinos G. San Diego: Elsevier, 2004, p. 407–435.
- Groh A, Bokor H, Mease RA, Plattner VM, Hangya B, Strohs A, Deschenes M, Acsady L. Convergence of cortical and sensory driver inputs on single thalamocortical cells. *Cereb Cortex* 24: 3167–3179, 2013.
- Jones EG. The thalamic matrix and thalamocortical synchrony. *Trends Neurosci* 24: 595–601, 2001.
- Jones EG. *The Thalamus*. Cambridge, UK: Cambridge University Press, 2007.
- Jones EG. Viewpoint: the core and matrix of thalamic organization. *Neuroscience* 85: 331–345, 1998.
- Kuramoto E, Fujiyama F, Nakamura KC, Tanaka Y, Hioki H, Kaneko T. Complementary distribution of glutamatergic cerebellar and GABAergic basal ganglia afferents to the rat motor thalamic nuclei. *Eur J Neurosci* 33: 95–109, 2011.
- Kuramoto E, Furuta T, Nakamura KC, Unzai T, Hioki H, Kaneko T. Two types of thalamocortical projections from the motor thalamic nuclei of the rat: a single neuron-tracing study using viral vectors. *Cereb Cortex* 19: 2065–2077, 2009.
- Lam YW, Cox CL, Varela C, Sherman SM. Morphological correlates of triadic circuitry in the lateral geniculate nucleus of cats and rats. *J Neurophysiol* 93: 748–757, 2005.
- Lam YW, Nelson CS, Sherman SM. Mapping of the functional interconnections between thalamic reticular neurons using photostimulation. *J Neurophysiol* 96: 2593–2600, 2006.
- Lam YW, Sherman SM. Different topography of the reticulothalamic inputs to first- and higher-order somatosensory thalamic relays revealed using photostimulation. *J Neurophysiol* 98: 2903–2909, 2007.
- Lam YW, Sherman SM. Functional organization of the somatosensory cortical layer 6 feedback to the thalamus. *Cereb Cortex* 20: 13–24, 2010.
- Lam YW, Sherman SM. Functional organization of the thalamic input to the thalamic reticular nucleus. *J Neurosci* 31: 6791–6799, 2011.
- Lam YW, Sherman SM. Mapping by laser photostimulation of connections between the thalamic reticular and ventral posterior lateral nuclei in the rat. *J Neurophysiol* 94: 2472–2483, 2005.
- Lee CC, Sherman SM. Topography and physiology of ascending streams in the auditory tectothalamic pathway. *Proc Natl Acad Sci USA* 107: 372–377.
- Lozsadi DA. Organization of cortical afferents to the rostral, limbic sector of the rat thalamic reticular nucleus. *J Comp Neurol* 341: 520–533, 1994.
- Montero VM, Guillery RW, Woolsey CN. Retinotopic organization within the thalamic reticular nucleus demonstrated by a double label autoradiographic technique. *Brain Res* 138: 407–421, 1977.
- Paxinos G, Watson C. *The Rat Brain in Stereotaxic Coordinates*. Oxford, UK: Elsevier Science, 2004.
- Schlag-Rey M, Schlag J. Visuomotor functions of central thalamus in monkey. I. Unit activity related to spontaneous eye movements. *J Neurophysiol* 51: 1149–1174, 1984.

Schlag J, Lehtinen I, Schlag-Rey M. Neuronal activity before and during eye movements in thalamic internal medullary lamina of the cat. *J Neurophysiol* 37: 982–995, 1974.

Schlag J, Schlag-Rey M. Visuomotor functions of central thalamus in monkey. II. Unit activity related to visual events, targeting, and fixation. *J Neurophysiol* 51: 1175–1195, 1984.

Shepherd GM, Pologruto TA, Svoboda K. Circuit analysis of experience-dependent plasticity in the developing rat barrel cortex. *Neuron* 38: 277–289, 2003.

Sherman SM, Guillery RW. *Thalamocortical Processing: Understanding Messages that link the Cortex to the World.* Cambridge, MA: MIT Press, 2013.

